Fen Bilimleri Dergisi, 24(2) (2012) 45-58.
Marmara Üniversitesi

http://dx.doi.org/10.7240/mufbed.v24i4.318

A metallographic examination of fracture splitting C70S6 steel used in connecting rods

Ziya AKSOY*, Zafer ÖZDEMİR, Tekin ÖZDEMİR

Balıkesir University, Department of Mechanical Engineering at Balıkesir, 10100, Balıkesir, TURKEY

Abstract:

Microalloyed high carbon steels (such as C70S6, SMA40 and FRACTIM) have been considered to be economic alternatives to powder metal and conventional steel, having been used as main crackable con-rod materials in recent years. Compared with powder metal and conventional steel, these microalloyed high carbon steels have remarkable advantages. One of the main advantages is that cost reduction can be achieved by changing the micro-structure of the con-rod. Sawing and machining processes of the rod and cap, in order to mate two faces can be eliminated, and is believed to reduce the production cost by 25%. Another advantage of this production method is that fracture-splitting connecting rods exhibit 30% higher fatigue strength and 13% less weight than conventional connecting rods, and can be splitted into two pieces (big body and cap) by fracturing with an instant impact load. Compared with powder metal and cast con-rods, it also has lower cost for the whole manufacturing process. Hence, it provides more advantageous production opportunities, and is prefered in manufacturing technology mostly. In this article, the metallographic and fracture surface analysis have been investigated using optical and SEM method. Hardness of C70 steel is also determined. In the article it has been made clear that, the microstructure of the fracture-split con-rod has a fine grain size with densely pearlite because of its high carbon content. Also it is shown that a high hardness value is determined approximately 280-300 HB. Almost no deformation exhibits after splitting into 2 pieces, which is what any con-rod productor would like to expect when utilizing C70S6 crackable steel in production phase.

Keywords: connecting rod, fracture splitting, metallographic examination, crackable C70S6 steel

1. Introduction

Until the advent of the crackable PF (powder forged) connecting rod cap end, all connecting rod cap ends had been sawn or machined apartly to enable inclusion of a bearing and attachment to the crankshaft [1]. With the recent introduction of new materials such as C70S6, FRACTIM and SMA40 splittable steels into the con-rod production process, powder metal connecting rods have lost their advantage. Nowadays, some automotive manufacturers have started to switch their production method from PM to forged steel connecting rods due to the advantages which newly-found methods provide higher strength and lower manufacturing costs. In addition to this, compared with the powder metal, better fatigue resistance of the forged steel has also been observed. Long-life fatigue strength at 10^6 cycles of the forged steel is 27% higher than that of the powder metal. The C70S6 steel exhibits equivalent fatigue strength compared to powder metal in the high cycle regime. Based on strain-life

*Sorumlu yazar: Ziya AKSOY, zaksoy@balikesir.edu.tr

fatigue behavior, the forged steel provides a factor of 7 times longer life than the powder metal in the high cycle regime. Accordingly, at short cycle regime the difference becomes smaller. On the other hand, the C70S6 steel (Fig.1) exhibits similar strain-life resistance, as compared to powder metal in the high cycle regime. [2-4]

Fig. 1. Forged C70S6 Steel [2]

The chemical composition of C70S6 steel (Table 1) is detailed below.

Table 1. Chemical composition of fracture splitting steel (%) [2]

Designation %	C	Si	Mn	P	S	Cr	V	Ni	Fe
C70S6	0.692	0.182	0.507	0.02	0.064	0.114	0.042	0,060	Remain

1.1. Purpose and the content of the study

In this article it is aimed to observe the mechanical behaviour of the fracture and the properties of the microstructure. Also it is aimed to understand the effect of this sudden (instant impact force) fracture to the mechanical properties. The metallography of the fracture surfaces have shown us that the fracture is a proper brittle fracture. As the fracture experiments go on, we have seen that the fracture surfaces exactly fit each other resulting with no material loss.

The study consists of fracture analysis, metallographic observation and the interpretation of these analysis. The hardness has been measured, the relation of the hardness and microstructure has been examined.

1.2. Findings in literature

Material composition of crackable con-rod steels are on the table below (Table 2); C70S6, SM40A and FRACTIM. On the microscopic photos the pearlitic structure can be seen appearently.

Table 2. Chemical compositions of materials used as crackable con-rod steels (weight %, nominal).

Specification	C	Si	Mn	P	S	Ni
C70S6	0.69	0.18	0.50	0.020	0.064	0.060
FRACTIM	0.63	0.25	0.76	0.042	0.088	0,025
SMA40	0.39	0.51	0.92	0.003	0.048	0.031

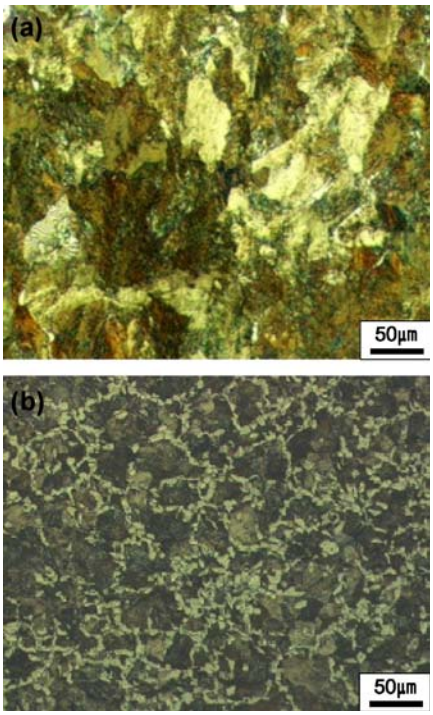

Fig.2. Optical micrograph of heat treated specimens (a) C70S6 and (b) SMA40. [5]

Microstructure of test specimens by optical microscope is shown in Fig.2 after etching in 3% nital solution. In general, both specimens mostly contain of pearlite, mixed with small amount of ferrite. More ferrite is found in SMA40 sample since it has lower carbon content than C70S6. [5]

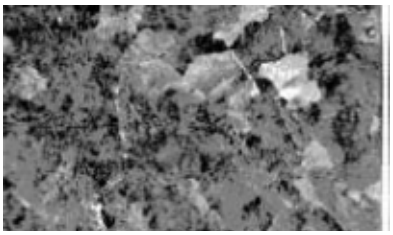

C70S6 x200

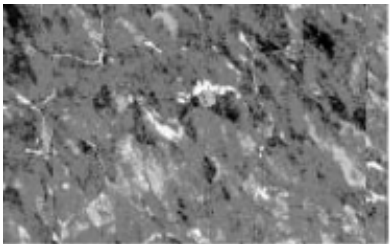

FRACTIM® x200

Fig. 3. Microstructures of C70S6 and FRACTIM® [6]

For obtaining minimum distortion of the big end in fracture splitting, it is a desired factor that the steel has densely pearlitic microstructure. By the use of higher Mn level in FRACTIM®, it is achieved with a lower C content and a slight increase in the amount of ferrite compared with C70S6; see Fig. 3 [6]

Table 3 Microstructure and grain dimension under various rolling processes

Process	Microstructure	Percent of pearlite %	Lamellar spacing of pearlite / µm	Grain size of ferrite / µm
1	Pearlite + ferrite	64	0,22	7,5
2	Pearlite + ferrite	74	0,19	6,0

Table 4 Hot rolling processes

Process	Reheating Temp/°C	Entry Temp of Finish Rolling /°C	Finish Temp/°C	Cooling rate /°C/s
1	1200	980	950	1.5
2	1200	980	930	15

The fraction volume of pearlite is shown in Table 3, mean linear intercept grain sizes of ferrite, and lamellar spacing of pearlite in the microalloyed steel under as-received condition. It was obvious that the volume fraction of pearlite increased approximately 15% and the mean linear intercept grain sizes of ferrite is reduced approximately 20% by reducing the finishing rolled temperature and accelerating the cooling rate (Table 4). Furthermore, lamellar spacing of pearlite is reduced 14% in Process 2. [7-10]

As Xianzhong. Zhang., Qingfeng. Chen., Qizhou. Cai., Guifeng. Zhou., Yuzhang. Xiong stated [7] that, the basic difference between Process 1 and Process 2 is deformation temperature during finish rolling and cooling rate after finish rolling. Decrease in the deformation temperature leads to a decrease in the austenite grain size, and an increase when transforming to ferrite. At these conditions, transformation from austenite to ferrite or pearlite is promoted due to the increase in nucleation sites at grain boundaries. Therefore, finer ferrite grain sizes and shorter lamellar spacing of pearlite are obtained as is shown in Fig. 4 [7]. Chemical composition of V-Ti-N Low Alloy Steel is shown in Table 5.

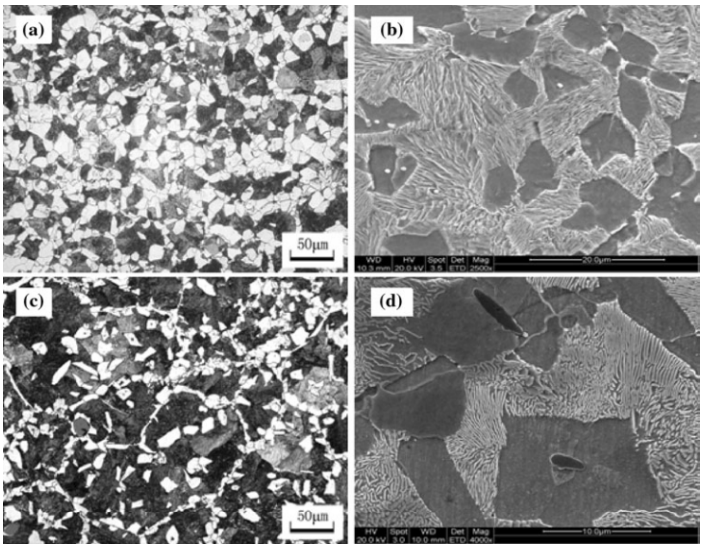

Fig.4. Microstructures of V–Ti–N microalloyed medium carbon steel a Optical photo, Process 1; b SEM, Process 1;c Optical photo, Process 2; d SEM, Process 2 [7]

Table 5 Chemical composition of v-ti-n microalloyed steel (wt %)

C	Si	Mn	P	S	Cr	V	Ti	N
0,36	0,66	1,00	0,010	0,045	0,27	0,26	0,013	0,0110

According to Zhang [7] SEM observations show that fine particles were precipitated in the ferrite (Fig. 1b and d), later identified as V(C, N) or (V, Ti) (C, N). The V(C, N) or (V, Ti) (C, N) particles restrict the prior austenite grain size and decrease the proeutectoid ferrite grain size because an increase in amount of grain boundaries improves proeutectoid ferrite nucleation [7]. These fine particles cause more tough and strong structure so as to ensure proper connecting rod running.

2. Examination

Our study consists of; 1) Fracture splitting experiment of C70S6 steel (Fig. 5) and visual examination, 2) Optical metallographic examination 3) SEM (Scanning Electron Microscope) Analysis, 4) Hardness Measurement.

2.1. Fracture splitting experiment and visual examination of the fracture

Fig. 5. C70S6 crackable con-rod used in experiments

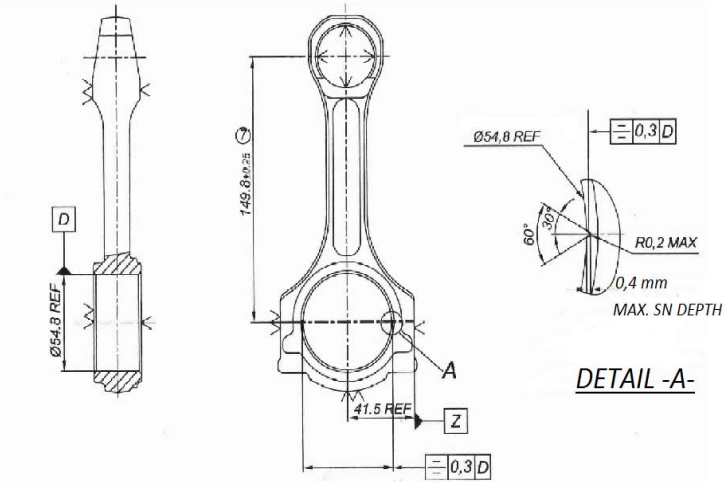

Fig. 6. Crackable Connecting Rod Used In Experiments

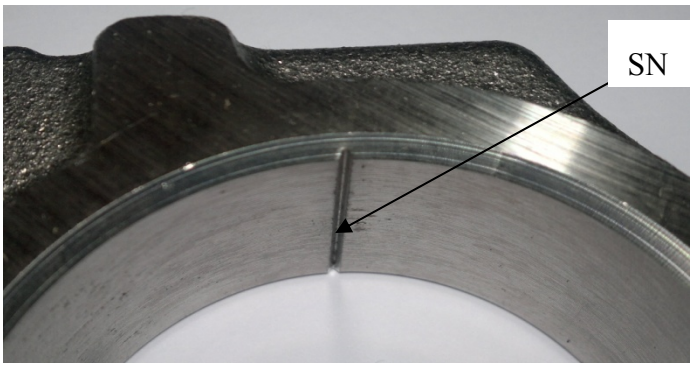

Fig. 7. Starting-Notch (SN) of crackable con-rod C70S6

The hydraulic pressure used in fracture splitting experiment is 160000 kg. The connecting-rod has been split into two pieces with an impact load. The load and velocity parameters are 1600 kN and 330 mm/s.

A technical drawing con-rod used in experiments is shown in Fig. 6. SN (Fig.7) is the first initiation point of the crack and a perfect match could be obtained after the fracture (Fig.8). We have obtained a one-impact fracture. As SN depth increases, the fracture pressure decreases, but 0,1-0,4 mm. is optimum.

Starting notch is an important fracture parameter. Experimental results show that the proper notch depth scale of the con/rod lies between 0.4 - 0.6 mm. In production, it is found that a proper scale of notch width or notch bottom radius is 0.1 - 0.4 mm. [10,11]

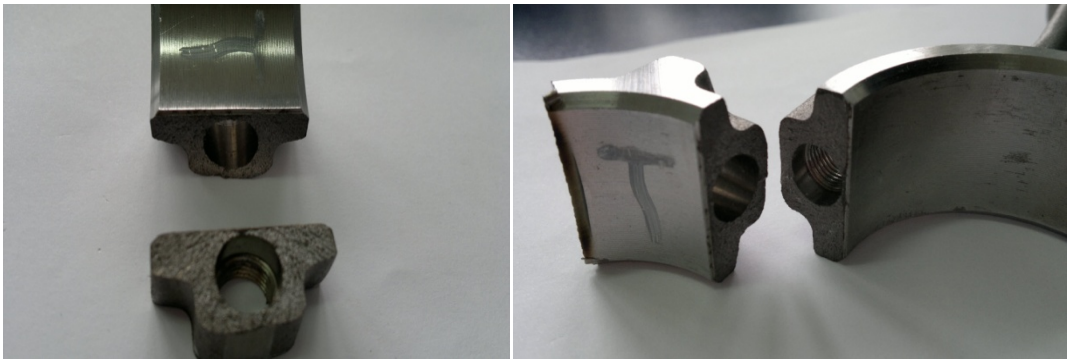

Fig. 8. Fractured faces

2.2. Optical photography

The fracture surface of the connecting rod was examined in the Nikon MA 100 Metal Microscopy and chemical analysis has been examined by BAIRD DVG Spectrometer. Hardness measurement has been done by Brinell Hardness Measurement Equipment.

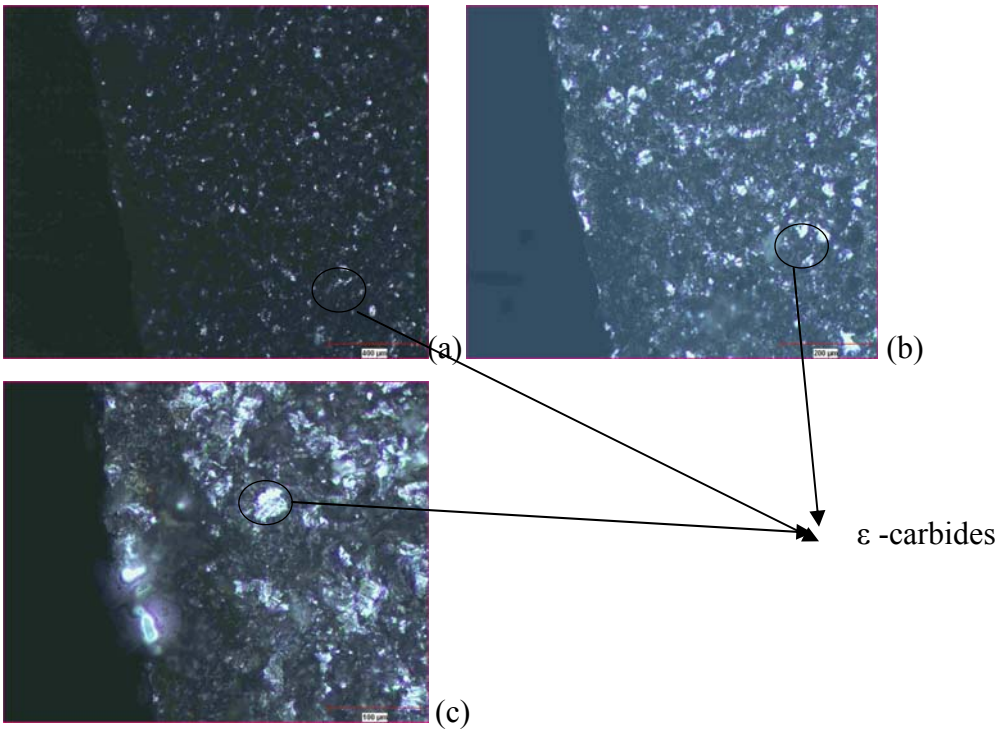

Fig. 9 (a) **Fracture surface, brittle and non-deformation fracture**

(b, c) **Fracture surface fine lamellar pearlite matrix (black) and ferrite (white)**

The microstructure in these photos is typical for high carbon steel, with a fine lamellar pearlite matrix (Fig. 9a), inserts of ferrite (Fig. 9b) (approximately 10 %) and ε carbides (Fig. 9c) could be seen.

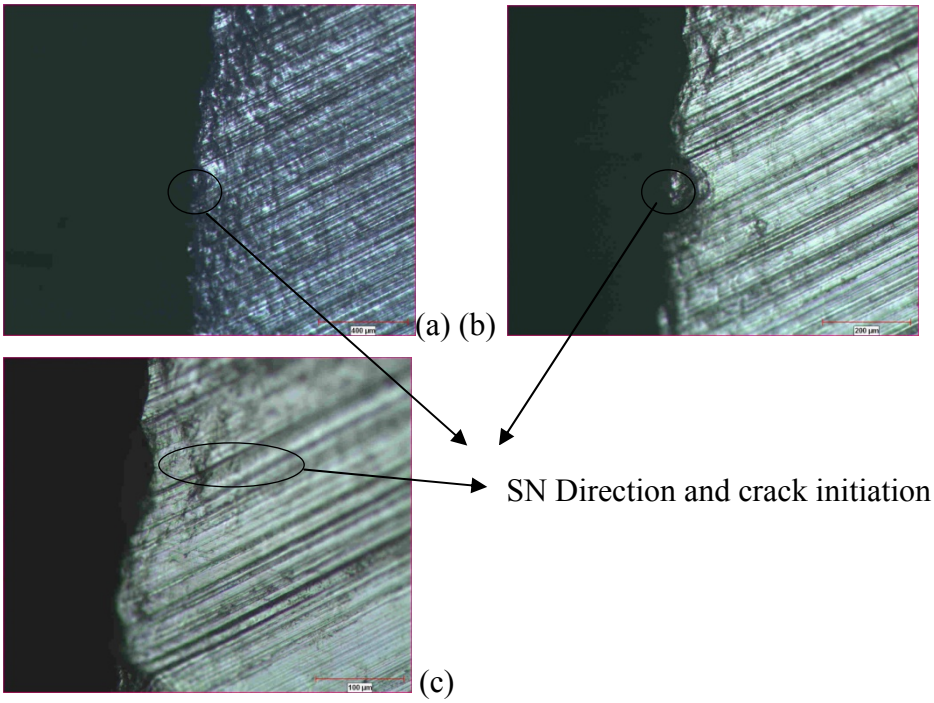

Fig. 10. (a,b,c) **Starting notch direction and brittle fracture starting**

Fracture occurs suddenly and brittle (Fig.10a). It is apparently seen that there is no-deformation (Fig.10b) and material loss in optical examination and experiments (Fig.10c).

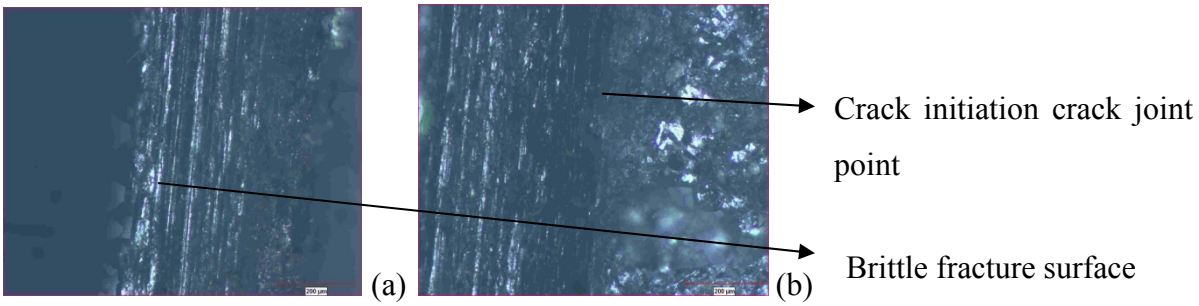

Fig. 11. (a,b) **Crack initiation and surface-crack point joint**

Also crack initiation point (Fig. 11a) and a brittle fracture surface (Fig. 11b) can be seen.

2.3.SEM analysis

The SEM analysis is done by using a JEOL/JSM-6510 LV scanning electron microscopy. As seen in photos below, the fracture is a brittle fracture-granular fracture (also cleavage fracture) and the microstructure consist of pearlite and ferrite with a dendritic structure without any production defect.

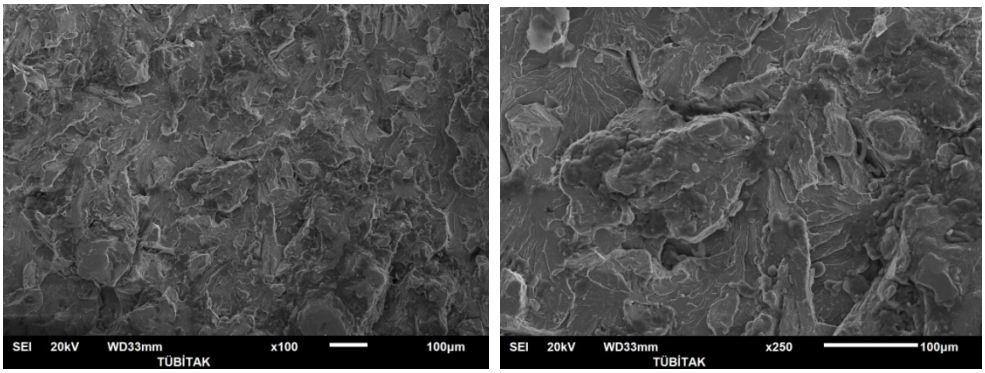

Fig. 12. SEM photo 1 (Dendritic fine pearlite and little ferrite could be seen obviously)

Fine pearlite particles could be seen clearly (Fig.12).

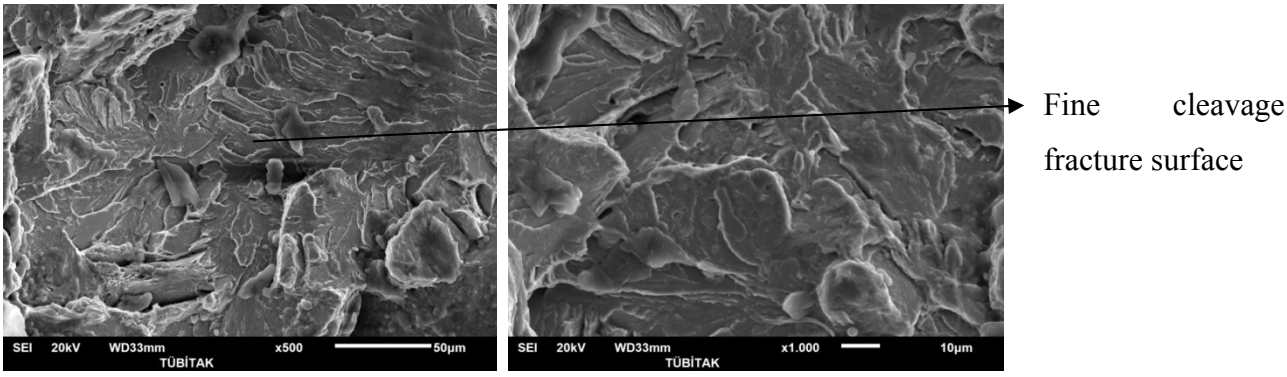

Fig. 13. SEM photo 2 (A cleavage (intergranular) and brittle fracture surface could be seen)

A perfect cleavage fracture surface could be seen (Fig.13).

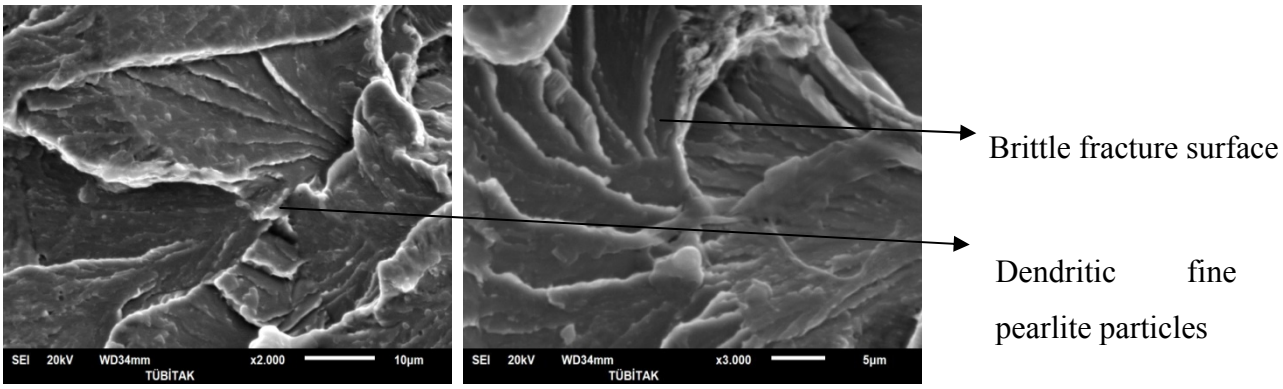

Fig. 14. SEM photo 3 (Dendritic fine pearlite particles could be seen)

Dendritic fine pearlite and brittle fracture surface could be seen obviosly (Fig. 14).

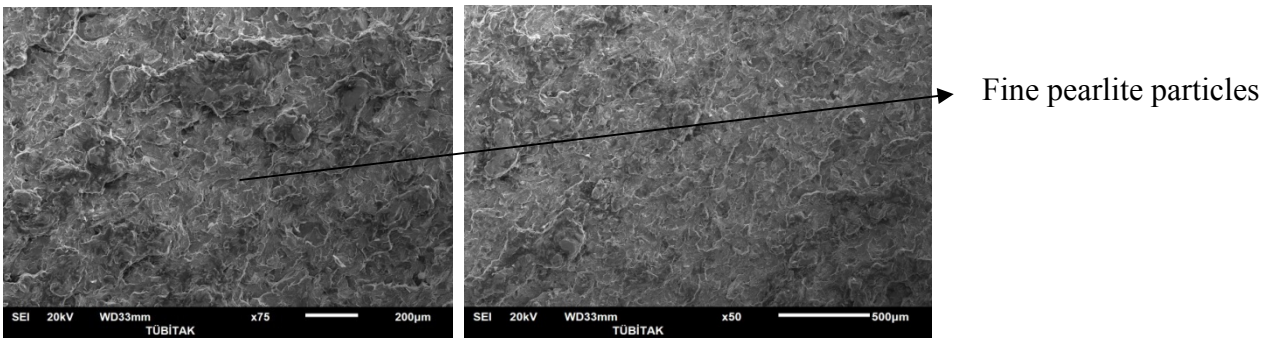

Fig. 15. SEM photo 4 (Fine pearlite and little ferrite)

SEM observations have showed that fine lamellar and grain size pearlite has occurred in the microstructure mostly. The microstructure is homogeneous and continuous (Fig.15).

2.4. Hardness, mechanical properties and chemical analysis

Hardness value is measured (Fig.16) between the value of 280 – 310 HB.

Fig. 16. Face used in spectral analysis and hardness measurement

The chemical composition (Table 6) and some important mechanical properties of C70S6 steel (Table 7) used in experiments are detailed below.

Table 6. Chemical composition of the crackable C70 steel used in the experiments

Comp.	C	P	Mo	Si	S	Ni	Mn	Cr	Al	V	Fe
%	0,692	0,01	0,015	0,182	0,064	0,072	0,507	0,114	0,003	0,042	Remain

Table 7. Some important mechanical properties of the C70 steel used in the experiments

σ yield [MPa]	σ max [MPa]	Hardness [HRB]	% ε Elongation
560	850-1100	280-310	10

The fraction of pearlite Wp (pearlite weight) may be determined according to; [12]

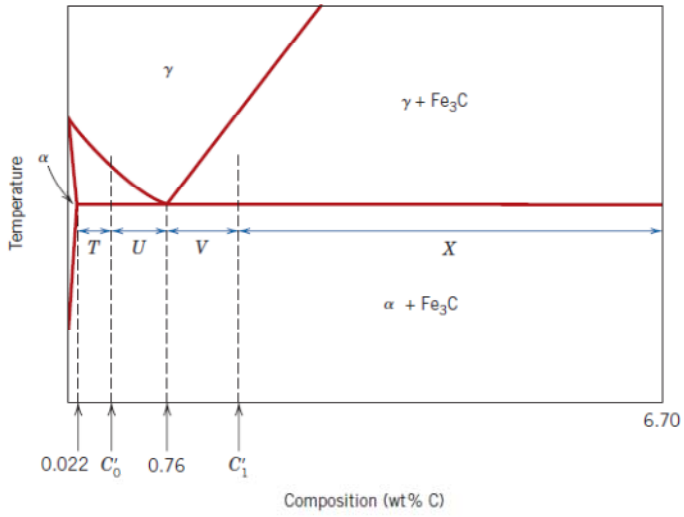

Fig. 17. A portion of the Fe–Fe3C phase diagram used in computations for relative amounts of proeutectoid and pearlite microconstituents for hypoeutectoid(C'_0) and hypereutectoid (C'_1) compositions. [12]

The relative amounts of the proeutectoid ferrit and pearlite may be determined in a manner according to that described in Fig. 17. Lever rule expression for computation of pearlite mass fraction (composition Figure 9.31) C'_0., here C'_0 =0,692 (carbon content in C70S6);

$$Wp = \frac{T}{T+U} = \frac{0,692 - 0,022}{0,76 - 0,022} = 0,90786$$

Lever rule expression for computation of proeutectoid ferrite mass fraction;

$$W\alpha = \frac{U}{T+U} = \frac{0,76 - 0,692}{0,76 - 0,022} = 0,09214$$

Here, 0,76 is the eutectoid point according to Iron-Iron Carbide Equilibruim Diagram, 0,022 is the % Carbon content of %100 ferrite according to Iron-Iron Carbide Equilibruim Diagram from here; approximately % pearlite is 0,91 and % ferrite is 0,09 [12].

3. Results

The microstructure in the examples given above is typical for high carbon steel, with a fine lamellar pearlite matrix and small inserts of ferrite (approximately 9 %) around the graphite nodules (Figs. 9 -15). This microstructure is hard and strong because of highly pearlite amount.

A granular fracture is obtained and it is a cleavage fracture also. SEM photos show that the structure is dendritic and the optical photos show that the ε-carbides are also in the structure. The ε-carbides ensure a more compact and fine structure so as to obtain a tough and strong con-rod.

The microstructure is mostly pearlite, so less ductile and more brittle structures can be obtained. For crackable con-rod materials, it is the desired structure. Furthermore, undesired effects of casting and powder forging such as inclusions and porosity can be eliminated by this way. The structure is homogeneous and continuous as seen in both optical and SEM photos. This is important and a desired factor for a con-rod works under different kinds of forces.

High carbon and low alloy C70S6 steel can highly obtain a hard structure so as to ensure a brittle fracture; tough and strong structure so as to ensure a high performance crackable con-rod running.

3.1. Effects of alloying elements :

Ratio of Mn in the element causes an increasing effect on impact toughness and it is not desired much for crackable con-rods.

Ratio of S in the element provides machinability and brittleness and its ratio is slightly more than conventional steels.

Ratio of C has the determinant effect on hardness and brittleness. Toughness and impact energy is inversely proportional with carbon ratio.

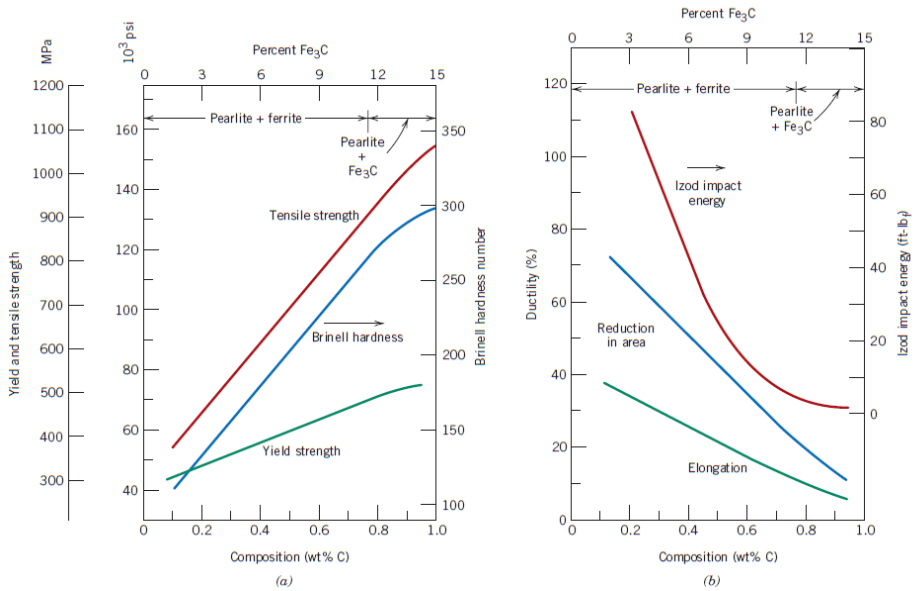

Fig. 18. (a) Yield strength, tensile strength, and Brinell hardness versus carbon concentration for plain carbon steels having microstructures consisting of fine pearlite.
(b) Ductility (%EL and %RA) and Izod impact energy versus carbon concentration for plain carbon steels having microstructures consisting of fine pearlite. [12]

As seen in Fig. 18, according to the increase in carbon content, hardness increases and impact energy decreases dramatically because of consisting fine pearlite grains. This microstructure is appropriate for crackable con-rods.

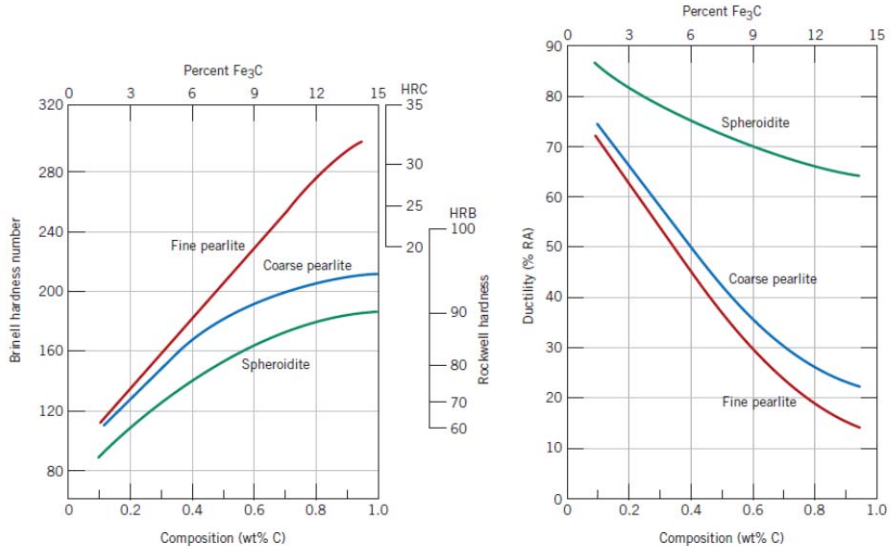

Fig. 19. (a) Brinell and Rockwell hardness as a function of carbon concentration for plain carbon steels having fine and coarse pearlite as well as spheroidite microstructure
(b) Ductility (%RA) as a function of carbon concentration for plain carbon steels having fine and coarse pearlite as well as spheroidite microstructures.

It could be inferred from Fig.19. that the ratio of ductility decreases as carbon and pearlite ratio increases. % 0,7-0,8 carbon content is approximately the optimum content of pearlite as seen in Fig. 19.a.[12]

4. Discussion

Material suitable for crackable con-rod must fulfill the needs for having fracture splitting capability, mechanical performance and also acceptable machinability. Mechanical performance is related to hardness and high hardness yields high performance. Hardness has adverse effect on machinability [13]. To overcome this opposite effect; crackable C70S6 steel has high carbon rate (% 0,692) for high hardness. S (sulfhur) content is higher (%0,06) than conventional low alloy (% 0,04) high carbon steels to ensure proper machinability.

As seen in both optial and SEM analysis, a proper cleavage fracture surface is obtained. Decreasing the content of Mn and N and increasing the content of Si and V, we can gain lower ductility and higher brittleness [10].

The composition is mostly pearlite (%91). We have neither a martenzite nor a ferritic microstructure. So the composition of material (C70S6) used in fracture splitting connecting rods has proper hardness (280-300 HB.) and strength ($\sigma_{max.}$=850-1000 MPa) values.

Changing the microstructure with various heat treatment applications (austempering) harder and tougher microstructure like bainite could be obtained and used in fracture splitting experiments. This can be another research area for fracture splitting parameters.

5. Conclusion

The fractured connecting rod has a microstructure of pearlite-ferrite brittle iron with a normal size and shape of fine pearlite as well as a normal hardness of 280-300 HB. The ratio of ferrite is approximately 10 % of the content. The morphology of the fracture surface indicates that the fracture occurres instantaneously.

It is concluded that;
1. The fractured connecting rod has a microstructure of pearlite ferrite brittle iron with a normal size and shape of graphite nodules as well as a normal hardness of 280-300 HB. The ratio of ferrite is 9 %, and pearlite is % 91 approximately.

2. Undesired effects of casting and powder forging like inclusions and porosity can be eliminated.
3. The material C70S6 used is appropriate to use crackable con-rods.
4. Considering the impact fracture surface of the developed high carbon microalloyed steel, it is easy to obtain a brittle fracture due to the high strength and certain amount of MnS, and small amount of carbonitride with oxide particles, which can become the cleavage initiation.
5. Optimum carbon ratio for fine pearlite is determined as %0,7 – 0,8.
6. As seen in optical and SEM observations, the fracture is cleavage, brittle and intergranular; fine pearlite grains are observed.
7. ε carbides could be seen in the structure, this is a result of a more brittle fracture.
8. Finally; the microstructure is homogeneous and continuous as observed in optical and SEM photos. The connecting rod should be designed with high reliability. It must be capable of transmitting axial tension, axial compression, and bending stresses caused by the thrust and pull on the piston, and by centrifugal force without bending or twisting. So this homogeneous and continuous structure is a desired factor for a con-rod.

REFERENCES

[1] James, R. Dale., Connecting rod evaluation, **Metal powder industries federation**, Princiton, (2005).
[2] Afzal, A., Fatigue behavior and life predictions of forged steel and powder metal connecting rods, Master Thesis, University of Toledo, Mechanical Engineering, Toledo, (2004).
[3] Repgen B., Optimized connecting rods to enable higher engine performance and cost reduction, **SAE technical paper series**, Paper No:980882, (1998).
[4] Pravardhan, S., and Fatemi, A., Connecting rod optimization for weight and cost reduction, **SAE International**, University of Toledo, Toledo, (2005).
[5] Hye. Sung. Kim., Tae. Gyu. Kim., Tai-Joo. Chung., Hyun. Soo. Kim., Soon-Jik. Hong., Fatigue characteristics of high strength C70S6 and SMA40 steels, Materials Science and Engineering, A 527 2813–2818, (2010).
[6] Corus Engineering Steel, FRACTIM, An improved machinable air cooled fracture splittable carbon steel for connecting rods. (2003).
[7] Xianzhong. Zhang., Qingfeng. Chen., Qizhou. Cai., Guifeng. Zhou., Yuzhang. Xiong., Microstructure and mechanical properties of V-Ti-N microalloyed steel used for Fracture splitting connecting rod, J Mater Science 46:1789–1795 (2011).
[8] Shanmugam S. Ramisetti NK., Misra RDK et al Mater Science Eng. A 460–461:335, (2007).
[9] Li. Z., Wu. D., Lv. H-S., Fang. S-R., J Iron Steel Res., 14(5):277, (2007).

[10] Z.Gu., S.Yang., S. Ku., Y. Zhao., X. Dai., Fracture splitting technology of automobile engine connecting rod, Int J Adv Manuf. Springer-Verlag London Limited, 25: 883–887, (2005).

[11]Ai. JH., Zhao. TC., Gao. HJ., et al J Mater Process Technol., 160 (3):390, (2005)

[12] William. D. Callister., JR. Salt Lake City, Material Science and Engineering, The University of Utah, (2006).

[13] Roland W III., Ian H., Nagarjuna N., Sven B., Anders B., Hoganas AB., New materials for powder forged connecting rods, Powder Met.2009, Las Vegas USA, (2009).